PHYSICS AND CHEMISTRY OF SOLID STATE

V. 26, No. 2 (2025) pp. 344-349

Section: Physics

DOI: 10.15330/pcss.26.2.344-349

Vasyl Stefanyk Precarpathian National University

ФІЗИКА І ХІМІЯ ТВЕРДОГО ТІЛА Т. 26, № 2 (2025) С. 344-349

Фізико-математичні науки

PACS: 78.30.Jw; 78.67.Pt; 78.55.Et ISSN 1729-4428 (Print) ISSN 2309-8589 (Online)

F.F. Sizov and Z.F. Tsybrii

Optical transmittance of CdTe/HgCdTe/CdZnTe structures

V.E. Lashkaryov Institute of Semiconductor Physics, NAS of Ukraine, Kyiv, Ukraine, tsybrii@isp.kiev.ua

The infrared (IR) optical transmittance of the liquid phase epitaxy (LPE) mono-crystalline p-type MCT (Hg_{1-x}Cd_xTe (x \approx 0.28)) layers grown on (111) surface of dielectric single crystal substrates CZT (Cd_{0.96}Zn_{0.04}Te) having the same lattice constant as these epitaxial layers, was investigated. The infrared transparency characteristics of the uncoated MCT layers and those coated with thin (d \approx 410 nm) CdTe films in the spectral range of free carrier absorption were studied. The coated with CdTe MCT films shows the increase of transmission coefficients, which was quantitatively evaluated by the CdTe/MCT/CZT multilayered structures transparency characteristics in the air environment.

Keywords: HgCdTe LPE layers, CdTe cover layers, IR transmittance.

Received 23 December 2024; Accepted 14 May 2025.

Introduction

The narrow-gap mercury-cadmium telluride (MCT, Hg_{1-x}Cd_xTe) is not a novel material for IR detectors. However, despite the more than 60 years since its invention and initial synthesis [1], due to its exceptional physical properties it remains one of the most dominant and promising materials for the IR quantum cooled detectors with ultimate performance [2 - 4]. Important trends for MCT detectors are those that they can be used at elevated, compared to T = 78 K, temperatures with high performance characteristics, because of the positive thermal coefficient dE_{ρ}/dT , where E_{ρ} is the band gap. In any other semiconductor this coefficient is negative (band gap is decreasing with temperature, e.g., in InSb). In [5] it was shown that it is possible to design MCT photodiodes operating up to temperature T = 300 K with the performance parameters, limited only by the background radiation fluctuations, excluding fundamentally the diffusion current generated by Auger-1 recombination, which is limiting the IR detector parameters.

The performance of detectors based on narrow-gap MCT epitaxial layers strongly depends on the substrate material and its orientation as well. That is a reason why CZT substrates are among those the most frequently used due to their good matching with MCT epitaxial layers

lattice. The purposes of this research were the investigation of the optical transmittance of the LPE grown mono-crystalline $Hg_{1-x}Cd_xTe$ ($x\approx 0.28$, lattice constant $a_o=6.4620$ Å) layers on (111)B surface of dielectric single crystal CZT substrates having the same or very close lattice constant as these epitaxial layers. The p-type LPE MCT layers with this chemical composition ($x\approx 0.28$) are used for manufacturing of photodiode detector arrays for $\lambda\approx 3$ to 5 µm spectral region.

I. Spectral transmittance of MCT/CZT and CdTe/MCT/CZT structures

1.1. Experimental data

Spectral transmittance T at some wavelength λ is defined by the ratio of the transmitted radiation intensity $I(\lambda)$ to the incident intensity $I_0(\lambda)$ in a small interval of wavelengths around the central radiation wavelength λ , $T = I(\lambda)/I_0(\lambda)$. Here the measurement of spectral transmittance were fulfilled with a help of PerkinElmer Spectrum BXII infrared Fourier spectrometer based on a Dynascan single-beam scanning interferometer with a Ge/KBr beam splitter accepting radiation normal incidence (really at small solid angle of aperture). In this work, two types of samples were examined, namely, LPE MCT

layers grown on CZT substrates and the same layers coated with a protective CdTe films.

Good quality of the LPE grown $Hg_{1-x}Cd_xTe$ ($x \approx 0.28$) layers and CdTe/HgCdTe/CZT structures are proved by a large number of the interference patterns in the transmission spectra (Fig. 1).

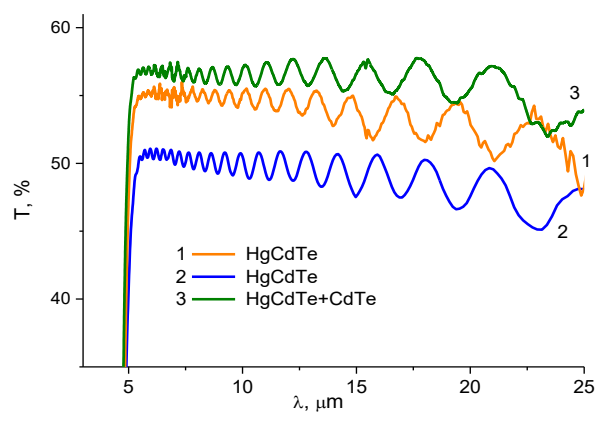


Fig. 1. Transmission optical spectra (T = 300 K) of the asgrown and with CdTe cover layer mono-crystalline $Hg_{1-x}Cd_xTe/Cd_{0.96}Zn_{0.04}Te$ structures (x = 0.278). For sample #1 from the interference spectra the thickness of the HgCdTe layer is $d_{MCT} \approx 16.3 \mu m$. For sample #2 the thickness of HgCdTe layer is close to the thickness of the layer in the sample #1.

These MCT monocrystalline epitaxial layers were grown on CZT dielectric substrates, which have a refractive index $n_{300}\approx 2.7$ [6]. The refractive index of $Hg_{1-x}Cd_xTe$ semiconductors depends much on chemical composition "x" and for layers with x=0.29 is $n(300~K)\approx 3.41$ [7]). This value of $n(300~K)\approx 3.41$ will be taken below in studying the $Hg_{1-x}Cd_xTe$ (x ≈ 0.28) LPE epitaxial layers. The high and low frequency dielectric constants for CdTe at T=300~K are $\epsilon_\infty=7.05\pm0.05,\,\epsilon_0=10.60\pm0.15$ [8].

As one can see from the transmission spectra (Fig. 1) the transparency coefficient of the MCT/CZT structure covered with thin CdTe film is increased. The transparency of different samples and their thicknesses can deviate a little that depends on the transparency of the CZT substrate grown by Bridgman method and the electrical characteristics of LPE layers.

The structural quality of MCT epitaxial layers is also confirmed by XRD measurements, where narrow peaks in 2θ – ω scans in the vicinity of (111)B reflex of LPE MCT epitaxial layers (FWHM \approx 45 arcsec) were observed.

The thickness of MCT LPE layers (d \approx 16.3 μ m) were obtained from the pronounced interference fringes in the transmission optical spectra and the thickness of CdTe layers (d \approx 410 nm) were obtained from Scanning electron microscope data (Fig. 2) at T = 300 K.

Low-temperature deposition (T \leq 100 C) [9] of CdTe thin protective films slightly changes the chemical composition at the near-surface thin layer of the initial MCT layer (Fig. 3), which, however, practically does not change the measured band-gap value at the half-height of the transmission maximum.

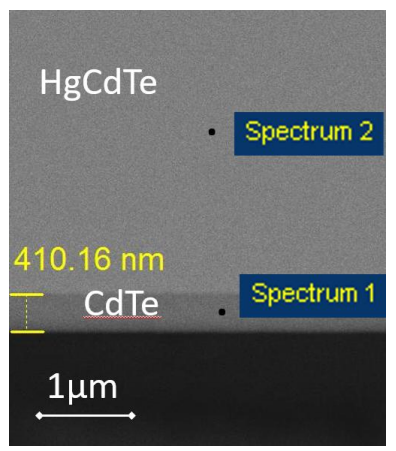


Fig. 2. Scanning electron microscope (TescanMira 3 MLU) photo of the CdTe/HgCdTe cleaved structure.

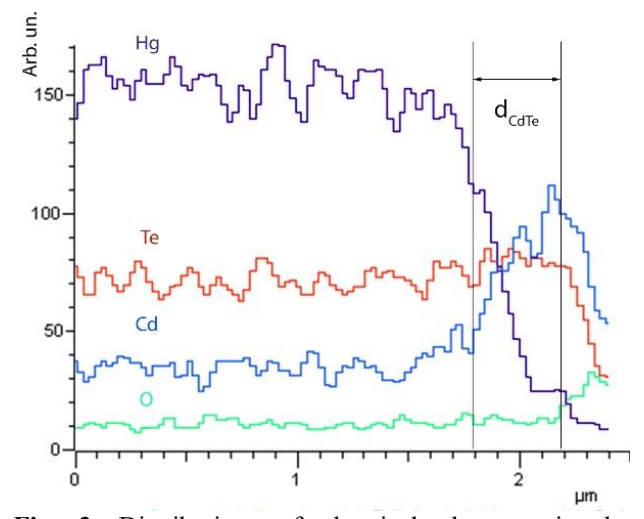


Fig. 3. Distributions of chemical elements in the $Hg_{0.72}Cd_{0.28}Te/CdTe$ cross section structure (EDX analysis, Oxford Instruments X-max).

Therefore, it will not practically change the cut-off wavelength of photo-response as at the typical value of the absorption coefficient in MCT layers $\alpha \sim 10^4~\text{cm}^{-1}\,[10]$ the depth of intensive absorption is about $2-2.5~\mu m$ (from $\alpha \cdot d \sim 2)$ where the chemical composition can be changed with depth. However, annealing at elevated temperatures significantly contributes the Hg atoms diffusion into the CdTe layer and leads to occupation the lattice positions of the Cd atoms, thus forming the HgCdTe structure [11].

2.2. Transmittance of the multilayer semiconductor structures: CdTe/MCT/CZT

The Fresnel's transmittance is defined as $T = I/I_0$, where I_0 is the light energy falling on a body and I is the light energy passed a body, through a plane-parallel thick slab with the index of refraction $n_j = n_2$ in the slab and with the index of refraction of surrounding medium $n_i = n_1$. It can be calculated taking into account the primary reflected plane electromagnetic wave and those reflected in the slab as the result of multiple reflections (Fig. 4) (assuming that there is no damping, scattering, luminescence, etc.).

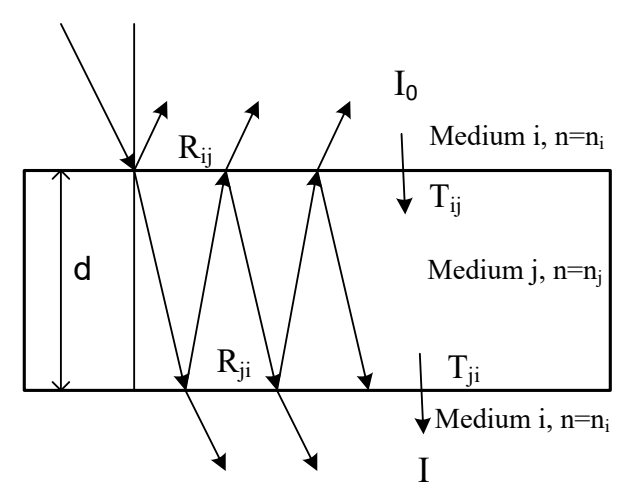


Fig. 4. Geometry of transmission and reflection of the plane-parallel transparent slab with refractive coefficient n_i in a media with the refractive coefficient n_i .

Assuming the absence of interference fringes as well and at normal radiation incidence, after the summation (see, e.g., [12]) the transmittance of a plane-parallel slab is

$$T = \frac{T_{ij} \cdot T_{ji}}{1 - R_{ji}^2},\tag{1}$$

where transmittance

$$T_{ij} = 1 - R_{ij} = T_{ji}, (2)$$

and reflectance

$$R_{ij} = R_{ji} = \left(\frac{n_j - n_i}{n_j + n_i}\right)^2.$$
 (3)

Fresnel's transmission coefficient T through a planeparallel sample imbedded in an air at radiation normal incidence assuming the radiation intensity (power) damping proportional to $\exp(-\alpha d)$ and in the case of neglecting interference effects but taking into account multiple reflections will be [12]

$$T = \frac{\left(1 - R_{ij}\right) \times exp\left(-\alpha_j(\lambda) \cdot d_j\right)}{1 - R_{ji}^2 \cdot exp\left(-2\alpha_j(\lambda) \cdot d_j\right)} \times \left(1 - R_{ji}\right),\tag{4}$$

where for reflectance (R_{ij} and R_{ji}) and transmittance (T_{ij} and T_{ii}), respectively Eqs. 2 and 3 are valid.

Here n_i and n_j are the indexes of refraction of the two contacted media and α is the absorption coefficient of a slab.

For the case of an air around both surfaces of a slab, $n_i = n_1 = 1$, $n_j = n_2 = n$, the reflection and transmission coefficients are $R_{12} = R_{21} = R$ and $\alpha_j = \alpha_2 = \alpha$, respectively, and then it follows the well-known Eq.

$$T = \frac{(1-R)^2 \times exp(-\alpha(\lambda) \cdot d)}{1-R^2 \cdot exp(-2\alpha(\lambda) \cdot d)}.$$
 (5)

For the case shown in Fig. 5, for multilayer structure with parallel interfaces at normal radiation incidence the transmission coefficient can be written as

$$T = (1 - R_{12}) \times \frac{exp(-\alpha_2 d_2)}{1 - R_{23}^2 \cdot exp(-2\alpha_2 d_2)} \times (1 - R_{23}) \times \frac{exp(-\alpha_3 d_3)}{1 - R_{34}^2 \cdot exp(-2\alpha_3 d_3)} \times (1 - R_{34}) \times \frac{exp(-\alpha_4 d_4)}{1 - R_{45}^2 \cdot exp(-2\alpha_4 d_4)} \times (1 - R_{45}).$$
 (6)

This Eq. considers multiple internal reflections in three-layer structure imbedded in an air environment. Here, it will be taken $\alpha(\lambda)=\alpha_{fea}(\lambda),$ where $\alpha_{fea}(\lambda)$ is the absorption coefficient of free carriers at certain $\lambda,$ as below we will consider only this kind of absorption. It is taken that for air $n_1=n_5=1,$ $\alpha_1=\alpha_5=0,$ then

$$\exp(-\alpha_1 d_1) = \exp(-\alpha_5 d_5) = \exp(-2\alpha_1 d_1) = \exp(-2\alpha_5 d_5) = 1.$$

Similar considerations of optical transmission in matrix notation through the planar multilayer structures at radiation normal incidence, not taking into account the interference effects as well, but with taking into account multiple internal reflections, were undertaken in [13].

In the case of sufficiently small absorption, the internal transmission can be indicated as [14]

$$T_{int} = exp(-\alpha \cdot d). \tag{7}$$

Then, in the case of the transmission through the boundary MCT/CZT, which are the materials with large refractive indexes but the small difference between them and small α ·d value in MCT layer, this approximation can be well applied as at the boundary of MCT/CZT (the structure shown in Fig. 5), the reflection coefficient $R_{34} = (3.41-2.70)^2/(3.41+2.70)^2 = (0.71/6.11)^2 = 0.0135$ and $R_{34}^2 = 1.82 \cdot 10^{-4}$ in the denominator of Eq. (4). Even

at $\alpha_{fca}(\lambda = 10 \ \mu m) \approx 20 \ cm^{-1}$ and $d_{MCT} \approx 16.3 \ \mu m$, the coefficient $2\alpha_{fca}(\lambda) \cdot d \approx 0.0032$ and exp(-0.0032) = 0.997. Therefore, $R_{34}^2 \cdot exp(-2\alpha \cdot d) = 1.82 \cdot 10^{-4} \cdot 0.994 = 1.81 \cdot 10^{-4}$ and $(1 - R_{34}^2 \cdot exp(-2\alpha(\lambda) \cdot d)) = 0.999816 \approx 1$.

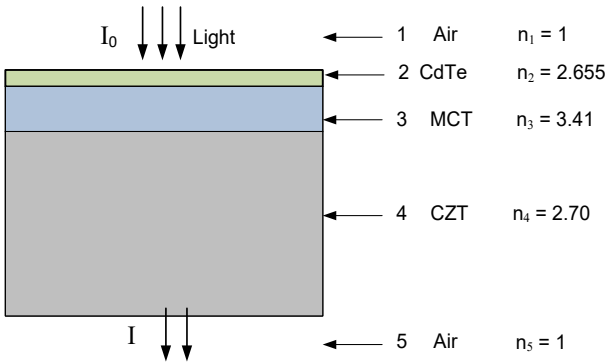


Fig. 5. Schematic of the air/CdTe/MCT/CZT/air multilayer structure.

The data of the refractive indexes "n" used here for estimations of radiation transmission through the MCT/CZT interface of the structure shown in Fig. 5 are cited in Table 1. Similar values of "n", which are close to this used data are given in the book [3].

Table 1. Refractive indexes used for the radiation transmission estimations through the structure shown in Fig. 5.

Semiconductor	$n = (\epsilon_{\infty})^{1/2}$	E _g , eV	Refs.	
CdTe	2.655	1.5	[8]	
Hg _{0.71} Cd _{0.29} Te	3.41	0.277	[7]	
Cd _{0.96} Zn _{0.04} Te	2.7	1.49	[6]	

However, such approximation (Eq. 7) for one-pass transmission without taking into account the denominator $[1 - R_{ji}^2 \cdot exp(-2\alpha_j(\lambda) \cdot d_j)]$ in Eq. 4 is less valid for semiconductors and dielectrics with a large difference between the refractive coefficients at the interfaces with air (small refractive index $n_{air} = 1$) (see Table 2).

One can see that with increasing difference between the indexes of refraction of a certain material, and other medium (here in an air) the deviation between the estimated transmission coefficients is growing up.

Table 2. Normal incidence transmittance for slabs of some materials in an air $(n_{air} = n_1 = 1)^*$.

Eqs.	Glass, $n_2 = 1.5$, in the visible	CZT, $n_2 = 2.7$, in the IR	Optical Si, $n_2 = 3.4$, in the IR
Eq. (5)	T = 0.923	T = 0.652	T = 0.541
Simplified Eq. (5) without R ² ·exp(-2αd) in the denominator	T= 0.9216	T = 0.623	T = 0.494

*It is taken $\alpha = 0$ for all the materials, which are considered as dielectrics.

In simplified expression for single-pass transmission of the structure shown in Fig. 5, without taking into account the denominators in Eq. 6, the transmission coefficient is

$$T = (1 - R_{12}) \times (1 - R_{23}) \times (1 - R_{34}) \times (1 - R_{45}) \times exp(-\alpha_2 d_2) \times exp(-\alpha_3 d_3) \times exp(-\alpha_4 d_4), \tag{8}$$

where for the R_{ij} reflection, indexes i, j=1...5 correspond to different layers, and where $n_1=n_5=1$ (air), $\alpha_1=\alpha_5=0$. This Eq. takes into account only the single-pass transmission through the 3 layers of structure embedded in an air.

For MCT layers without and with CdTe cover thin films there is observed the weak spectral dependences of transmittance in the range ($\lambda \sim 6-15~\mu m)$ out of the interband absorption at $\lambda < 5~\mu m$ (Fig. 1). This weak dependences of $T(\lambda)$ are mainly connected with the absorption of free carriers in MCT layers.

The free carrier absorption was estimated within the Drude model approximation using the static conductivity $\sigma_0 = e \cdot N \cdot \mu = N \cdot e^2 \cdot \tau/m^*$, where τ is the characteristic

relaxation time and $(\omega \cdot \tau)^2 >> 1$ that is valid for MCT semiconductor in the specified spectral range. Here $\omega = 2\pi \cdot c/\lambda$ is the angular frequency. Then, in this model, the absorption coefficient of free carriers is [15]

$$\alpha(\omega)_{fca} = \frac{N \cdot e^2}{n \cdot m^* \cdot c \cdot \varepsilon_0 \cdot \omega^2 \cdot \tau}.$$
 (9)

Here N is the concentration of free carriers, n is the refractive index, e is the electron charge, m* is the free carrier effective mass, c is the speed of light, $\epsilon_0=8.854\cdot 10^{-12}~\text{F/m}$ is the vacuum permittivity. Taking free carriers mobility as $\mu=e\cdot \tau/m^*,~\omega=2\pi\cdot c/\lambda$ and accepting two types of carriers (holes and electrons) it follows

$$\alpha(\lambda)_{fca} = \frac{e^3}{4\pi^2 c^3 \varepsilon_0} \times \lambda^2 / n \times \left[N_p / \mu_p \cdot \left(m_p^* \right)^2 + N / \mu_n \cdot (m_n^*)^2 \right], \tag{10}$$

which is the well known expression for free carrier absorption for two types of carriers [16]. Here m^*_p and m^*_n are the effective masses of holes and electrons respectively, N_p and N are the concentrations of free holes and electrons, respectively. The holes effective mass $m^*_p \approx 0.45 \cdot m_0$ [14], m_0 is the free electron rest mass, $m^*_n \approx 0.019 \cdot m_0$ for MCT with $x \approx 0.28$.

Here the intrinsic concentration $N_i(300 \text{ K}) \approx 6 \cdot 10^{15} \text{ cm}^{-3} \approx N$ for MCT with $x \approx 0.28$, was estimated using the expression for $N_i(x,T)$ in [17] and the mobility of free electrons was taken $\mu_n(300\text{K}) \approx 1500 \text{ cm}^2/\text{V} \cdot \text{s}$ as measured for n-type MCT layers ($x \approx 0.28$).

Using Eq. (10) there was estimated the free carrier absorption $\alpha(\lambda)_{fca} \sim 20~cm^{-1}$ by free holes and electrons at $\lambda \approx 10~\mu m$ in MCT layer (d_{MCT} $\approx 16.3~\mu m$). As CZT is a wide band-gap semiconductor (see Table 1) it was taken

for it $\alpha_{fca} \sim 0.25-1~cm^{-1}$ as $N_P < 10^{15}~cm^{-3}$ and there is vanishingly low intrinsic concentration. The thickness of CZT layer is $d_{CZT} \approx 800~\mu m$. These data were used for estimations of transparency of the air/CdTe/MCT/CZT/air and air/MCT/CZT/air structures (Table 3).

In the cap layer of a wide band-gap CdTe $E_g(300~K) \approx 1.5~eV,~N_P < 10^{15}~cm^{-3},~m^*_p \approx 0.45 \cdot m_0.$ Because of its thickness $d_{CdTe} \approx 410~nm \approx 4.1 \cdot 10^{-5}~cm$, the coefficient $\alpha_{fca} \cdot d$ is small, and $exp(-\alpha_{fca} \cdot d)$ as well as $exp(-2\alpha_{fca} \cdot d)$ are vanishingly small and can't be taken into account. In these semiconductors the hole mobility does not exceed the value $\mu_p \approx 90~cm^2/V \cdot s$ [18, 19] and, therefore, it can be taken $\alpha_{fca} \cdot d_{CdTe} \sim 0$. This value of $\mu_p(300~K)$ is a characteristic value for HgCdTe layers as well [20].

Table 3.

Transmission coefficients of "air/CdTe/MCT/CZT/air" and "air/MCT/CZT/air" structures at $\lambda \sim 10 \ \mu m$.

		T, %, experiment,	T, %, estimated,	T, %, estimated,			
	Structure	without interference	$\alpha(MCT)_{fca} \sim 20 \text{ cm}^{-1},$	$\alpha (MCT)_{fca} \sim 20 \text{ cm}^{-1},$			
		fringes	$\alpha(CZT)_{fca}\sim0.25~cm^{-1}$	$\alpha (CZT)_{fca} \sim 1 \text{ cm}^{-1}$			
	air/CdTe/MCT/CZT/air,	≈57	59.5	55.7			
	Eq. 6	~37	37.3	33.1			
	air/MCT/CZT/air, Eq. 6 (without CdTe film)	≈50 – 54, in dependence of the CZT substrate	54.1	50.6			
	air/CdTe/MCT/CZT/air, simplified Eq. 8,	≈57	57.7	54.4			

It was also supposed that for air $\alpha_1 = \alpha_5 = 0$ and, than $\exp(-\alpha_1 d_1) = \exp(-\alpha_5 d_5) = 1$.

From Table 3 it is seen that in the spectral range of free carriers absorption the transparency of coated with CdTe thin films MCT/CZT structures can be increased by about 5 % in the spectral range of free carrier absorption.

Conclusions

The optical transmittance spectra $T(\lambda)$ of p-type LPE grown mono-crystalline MCT layers on (111)B surfaces of dielectric single crystal CZT substrates were experimentally measured and analyzed. It was shown that $T(\lambda)$ characteristics of the MCT/CZT structures coated with thin (d \approx 410 nm) CdTe films deposited on MCT layers, exhibited an increase of transparency coefficients by several percent in the spectral range of free carriers

absorption. This increase of transparency was quantitatively explained by the transmittance of CdTe/MCT/CZT multilayered structures in the air environment, taking into account as the differences in the refractive indexes of the constituents and the absorption of free carriers as well.

Acknowledgements:

The authors are thankful to M. Vuichyk for carrying out some technological operations.

Funding:

This work was partly supported by the NAS of Ukraine, project No. III-10-24 and project No III-3-21.

Sizov F.F. – Corresponding Member of the NASU, Chief Researcher;

Tsybrii Z.F. – Doctor of Science, Head of department.

- [1] W.D. Lawson, S. Nielsen, E. H. Putley, A.S. Young, *Preparation and properties of HgTe and mixed crystals of HgTe-CdTe*, J. Phys. Chem. Sol., 9, 325 (1959); https://doi.org/10.1016/0022-3697(59)90110-6.
- [2] C.L. Tan, H. Mohseni, *Emerging technologies for high performance infrared detectors*, Nanophotonics, 7, 169 (2018); https://doi.org/10.1515/nanoph-2017-0061.
- [3] A. Rogalski, Infrared and Terahertz Detectors (Third Edition, CRC Press, 2019); https://doi.org/10.1201/b21951.
- [4] F. Sizov, Detectors and Sources for THz and IR (Materials Research Foundations, LLC Forum, Millesville, USA, 2020).
- [5] D. Lee, P. Dreiske, J. Ellsworth, R. Cottier, et al, *Law 19: The ultimate photodiode performance metric*, Proc. SPIE, 11407, 114070X-1 (2020); https://doi.org/10.1117/12.2564902.
- [6] M.A. Quijada and R. Henry, *Temperature evolution of exciton absorptions in Cd*_{1-x}*Zn*_x*Te materials*, Proc. SPIE, 6692, 669206 (2007); https://doi.org/10.1117/12.735604.
- [7] E. Finkman and S. E. Schacham, *The exponential optical absorption band tail of Hg_{1-x}Cd_xTe*, J. Appl. Phys., 56, 2896 (1984); https://doi.org/10.1063/1.333828.
- [8] O.G. Lorimor, W.G. Spitzer, *Infrared Refractive Index and Absorption of InAs and CdTe*, J. Appl. Phys., 36, 1841 (1965); https://doi.org/10.1063/1.171436.
- [9] F. Sizov, M. Vuichyk, K. Svezhentsova, Z. Tsybrii, S. Stariy, M. Smolii, *CdTe thin films as protective surface passivation to HgCdTe layers for the IR and THz detectors*, Mater. Sci. Semicond. Process, 124, 105577 (2021); https://doi.org/10.1016/j.mssp.2020.105577.
- [10] J. Chu, S. Xu, and D. Tang, *Energy gap versus alloy composition and temperature in Hg*_{1-x} Cd_xTe , Appl. Phys. Lett., 43, 1064 (1983); http://dx.doi.org/10.1063/1.94237.
- [11] J. Chen, Y. Lin, L. Li, et al, On the structural evolutionary behavior of the CdTe/HgCdTe interface during the annealing process, J. Mater. Research Technol., 28, 3175 (2024); https://doi.org/10.1016/j.jmrt.2023.12.185.
- [12] O. Stenzel, The Physics of Thin Film Optical Spectra (Ch. 7 "Thick slabs and Thin Films", p. 101 124, Springer, 2016).
- [13] S.H. Wemple and J.A. Seman, *Optical transmission through multilayered structures*, Appl. Opt., 12, 2947 (1973).

- [14] H.-J. Hoffmann, Optical Glasses in K. H. J. Buschow, R. W. Cahn, M. C. Flemmings, B. Ilschner, E. J. Kramer, S. Mahajan (eds.-in-chief), *The Encyclopedia of Materials: Science and Technology (EMSAT)*, ISBN 0-08-0431526 (Elsevier Science, Cambridge, 2001).
- [15] C. Ndebeka-Bandou, F. Carosella, R. Ferreira, A. Wacker and G. Bastard, *Free carrier absorption and inter-subband transitions in imperfect heterostructures*, Semicon. Scie. Technol., 29, 023001 (2014); https://doi.org/10.1088/0268-1242/29/2/023001.
- [16] R.A. Smith, Semiconductors (New York: Cambridge, 1961).
- [17] J.R. Lowney, D.G. Seiler, C.L. Littler, and I.T. Yoon, *Intrinsic Carrier Concentration of Narrow-Gap Mercury Cadmium Telluride*, J. Appl. Phys., 71, 1253 (1992); https://doi.org/10.1063/1.351371.
- [18] P.J. Sellin, A.W. Davies, A. Lohstroh, M.E. Özsan, and J. Parkin, *Drift mobility and mobility-lifetime products in CdTe:Cl grown by the travelling heater method*, IEEE Trans. Nucl. Sci., 52, 3074 (2005); https://doi.org/10.1109/TNS.2005.855641.
- [19] K. Suzuki; S. Seto; T. Sawada; K. Imai, Carrier transport properties of HPB CdZnTe and THM CdTe:Cl, IEEE Trans. Nucl. Sci., 49, 1287 (2002); https://doi.org/10.1109/TNS.2002.1039653.
- [20] Y. Gui, B. Li, G. Zheng, Y. Chang, et al, Evaluation of densities and mobilities for heavy and light holes in p-type $Hg_{I-x}Cd_xTe$ molecular beam epitaxy films from magnetic-field-dependent Hall data, J. Appl. Phys., 84, 4327 (1998); http://dx.doi.org/10.1063/1.368652.

Ф.Ф. Сизов та З.Ф. Цибрій

Оптичне пропускання структур CdTe/HgCdTe/CdZnTe

Інститут фізики напівпровідників ім. В.Є. Лашкарьова НАН України, Київ, Україна, tsybrii@isp.kiev.ua

Досліджено інфрачервоне (IЧ) оптичне пропускання монокристалічних шарів МСТ р-типу ($Hg_{1-x}Cd_xTe(x\approx0.28)$), вирощених методом рідкофазної епітаксії (LPE), на поверхні (111)В діелектричних монокристалічних підкладок СZТ ($Cd_{0.96}Zn_{0.04}Te$), що мають таку ж постійну решітки, як і ці епітаксійні шари. Досліджено характеристики інфрачервоної прозорості непокритих шарів МСТ та шарів, покритих тонкими ($d\approx410$ нм) плівками CdTe, у спектральному діапазоні поглинання вільними носіями заряду. Плівки МСТ з покриттям CdTe демонструють збільшення коефіцієнтів пропускання, що було кількісно оцінено за характеристиками прозорості багатошарових структур CdTe/MCT/CZT у повітряному середовищі.

Ключові слова: шари LPE HgCdTe, покривні шари CdTe, коефіцієнт пропускання в ІЧ-діапазоні.